# Connecting the Nanodots: Programmable Nanofabrication of Fused Metal Shapes on DNA Templates

M. Pilo-Pais,[†,#] S. Goldberg,[†,#] E. Samano,[‡,§] T. H. LaBean,[*,‡,∥,⊥] and G. Finkelstein[*,†]

[†]Department of Physics, [‡]Department of Computer Science, [∥]Department of Chemistry, and [⊥]Department of Biomedical Engineering, Duke University, Durham, North Carolina 27708

[§]Centro de Nanociencias y Nanotecnología, Universidad Nacional Autómona de México, Ensenada, B.C., México

Ⓢ Supporting Information

**ABSTRACT:** We present a novel method for producing complex metallic nanostructures of programmable design. DNA origami templates, modified to have DNA binding sites with a uniquely coded sequence, were adsorbed onto silicon dioxide substrates. Gold nanoparticles functionalized with the cDNA sequence were then attached. These seed nanoparticles were later enlarged, and even fused, by electroless deposition of silver. Using this method, we constructed a variety of metallic structures, including rings, pairs of bars, and H shapes.
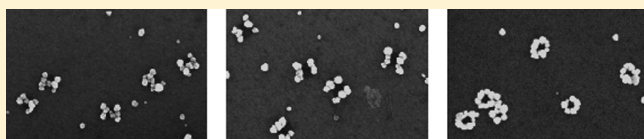
**KEYWORDS:** Nanoparticles, electroless deposition, DNA origami, self-assembly, nanofabrication, metallization

Nanoscale metallic structures hold great potential for both electronic and plasmonic applications. Their construction requires the controlled placement of metal with nanometer resolution and the ability to couple to the resulting structures, either electrically or optically. Fabrication of such structures is challenging and has pushed current lithographic techniques to their limits. For this reason, scientists have sought to self-assemble such nanostructures rather than use the conventional top-down approaches.

Artificial two-dimensional DNA assemblies provide a programmable methodology for bottom-up fabrication of complex nanostructures.[1,2] The flexibility and addressability of these systems have been greatly improved with the advent of "DNA origami", a method of creating arbitrary shapes and patterns on a ~100 nm scale.[3] The original origami is composed of an approximately 7-kilobase natural DNA strand (scaffold) and roughly 200 short synthetic cDNA strands, known as "staples." These staples fold the scaffold strand back upon itself and determine the shape of the origami. The staple strands can be further functionalized with various nanocomponents, making the origami a programmable breadboard for placement of other nanoscale objects. DNA origami has already been successfully used as a template for single-molecule chemical reactions,[4] placement of carbon nanotubes,[5] and DNA motors[6] and "walkers".[7,8] In addition, DNA origami has been used as a template for site-specific binding of gold[9−11] and silver[12] nanoparticles. It has also been demonstrated that DNA origami can be precisely positioned and oriented on microfabricated substrates, thereby providing a bridge between the lithographic and self-assembly methods.[10,13]

DNA can be metallized by reduction of metal ions from solution, resulting in formation of conducting wires.[14] Different metals have been deposited, including Ag, Cu, Pd, Pt, and Co (see ref 15 for a comprehensive review). Multistrand DNA assemblies have also been metallized, including DNA nanoribbons,[16] DNA nanotubes,[17] three-helix bundles,[18] and, very recently, DNA origami.[19] Alternatively, metallic nanoparticles, assembled using DNA, have been used as seeds for metallization.[20−25] However, in these works the reduced metal coated the entire structure and did not fully utilize the addressability of the underlying DNA template.

In this work, we combine the programmed placement of gold nanoparticles on DNA templates and their fusion by metallization. Our method allows us to create predesigned metallic structures such as rings, pairs of parallel bars, and H shapes with outer dimensions close to those of the DNA origami. Specifically, the seed nanoparticles are first attached to the DNA template at specific locations and then fused together by metal-on-metal deposition.

The previously reported "tall rectangle" DNA origami[3] (90 × 70 nm$^2$) was used as the DNA template for all of the metallic structures presented here. The origami was formed as originally designed by Rothemund,[3] but with the following changes: All of the side staples were left out to prevent aggregation via helix stacking interactions between adjacent origamis (see Supporting Information of ref 3). Additionally, two consecutive staples located at each of the AuNP binding sites were extended on the 3′ end by a short spacer sequence ($T_5$) followed by a specific 24 bp DNA sequence ($X_{24}$) (see Supporting Information for further details). The prepared origami (5 nM) was filtered by performing three buffer exchanges in 1xTAE/12.5 mM Mg$^{2+}$
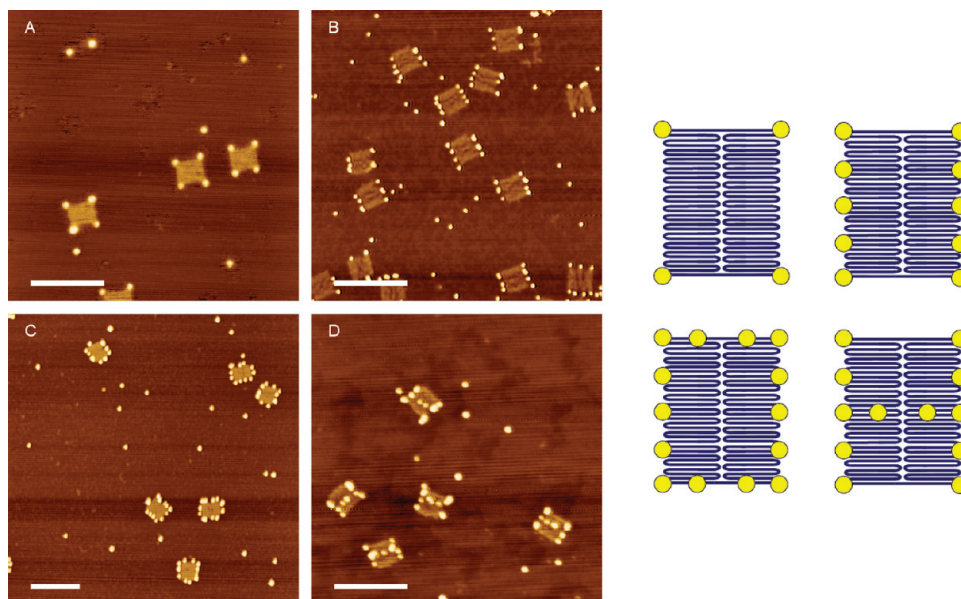
**Figure 1.** AFM images of different AuNP assemblies on mica: (A) four corners, (B) a pair of parallel bars, (C) ring, and (D) H shape. The patterns are programmed by extending different staples with the same complementary sequence, permitting the use of the AuNP–DNA conjugates for all assemblies. All scale bars are 250 nm. The size of the particles appears enlarged, due to convolution with the AFM tip. Schematic on the right shows the designed structures.

buffer (40 mM Tris-acetate, 1 mM EDTA, pH 8.2) with a single ultrafiltration centrifuge unit (100 kDa MWCO, Millipore) to remove the extra staple strands.

Gold nanoparticles (British Biocell International) of 5 nm were conjugated to a specific oligonucleotide chain ($X_{24,comp}$) at a AuNP:DNA ratio of 1:5 and allowed to incubate overnight, following the recipe of refs 26 and 27 and described in detail in the Supporting Information. The DNA strands used for conjugation were purchased from IDT (Integrated DNA Technologies, Inc.). They had a disulfide modification (lipoic acid) on the $5'$ end followed by a 5 base spacer ($T_5$) and the complementary sequence to that of the binding sites ($X_{24,comp}$). The AuNP–DNA conjugates were then backfilled with thiolated $T_5$ sequences (also from IDT) to prevent aggregation of AuNPs that would otherwise occur in the presence of ∼50 mM $Mg^{2+}$ ions; this incubation lasted 24 h at room temperature. Typical backfilling ratios ranged from 10:1 to 60:1 ($T_5$:AuNP). Unconjugated DNA strands were then removed from the AuNP–DNA conjugate solution using gel electrophoresis (3% agarose, 10 V/cm, 15 min run, 0.5xTBE). The AuNP–DNA conjugates were recovered from the gel using gel extraction columns (Squeeze and Freeze, Bio-Rad Laboratories, Inc.). We emphasize that we ran the conjugates on the gel for filtration purposes only, since 5 nm AuNPs conjugated to a 29-base sequence do not exhibit discrete bands. This filtration step greatly enhanced the yield of the AuNP attachment to the origami. We surmise that without this procedure, the unconjugated $X_{24,comp}$ strands saturate the binding sites on the origami. We find this protocol to be more efficient than using ultrafiltration centrifuge cartridges.[10]

We next placed the DNA templates on substrates. Mica (Ted Pella) and Si/SiO$_2$ (Silicon Quest, both native and 1 μm thick oxide) substrates were used in our experiments. Freshly cleaved mica was used for atomic force microscopy (AFM) imaging of both origami formation and gold binding (see Figure 1). For mica, the origami buffer was kept at 1xTAE/12.5 mM $Mg^{2+}$.
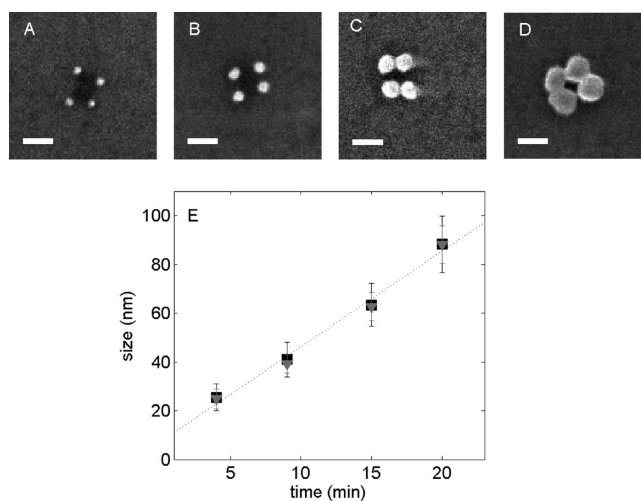


**Figure 2.** Controlled growth due to silver reduction of 5 nm AuNPs bound to the four corners of the rectangle origami. Metallization times: (A) 4, (B) 9, (C) 15, and (D) 20 min. All scale bars are 100 nm. (E) Average particle dimensions in horizontal (squares) and vertical (triangles) directions for different metallization times, as measured from SEM images.

Silicon was used for metallization and for scanning electron microscopy (SEM) imaging of the resulting structures (see Figure 3 below). Silicon substrates were cleaned by oxygen plasma ashing for 5 min at 100 W using a Emitech K-1050X, or at 80 mA using an SPI Plasma Prep II. Results for the two plasma ashers were similar. The origami solution was adjusted to 1xTAE/100 mM $Mg^{2+}$ in order to promote attachment of the DNA to the silicon dioxide susbtrate.[13]

On both types of substrates, the origami (0.5 nM, 5 μL) was deposited onto the surface and allowed to adsorb for 5 min. A
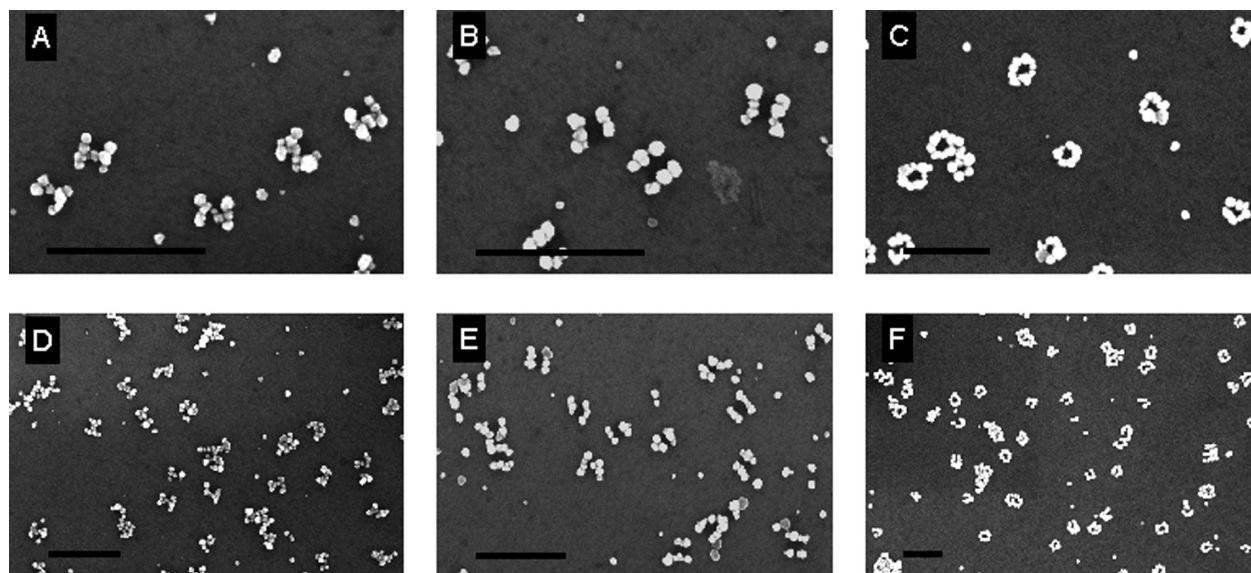
**Figure 3.** SEM images of different metallic nanostructures: (A) and (D) H shapes, (B) and (E) pairs of parallel bars, (C) and (F) rings. All scale bars are 500 nm.

solution containing functionalized AuNPs (15−100 nM) was then added and the samples were allowed to incubate at room temperature for an additional 30 min. The sample was then washed by immersing the substrate into deionized water (18 MΩ) for 10 s to remove excess unconjugated AuNPs and dried gently under a stream of nitrogen. Unlike ref 10, in our case it was not necessary to anneal the samples at elevated temperature or to incubate them for longer periods of time in order to obtain good binding.

We programmed different AuNP binding sites by extending different subsets of staples from the original "tall origami" staple set. The extension sequence was $X_{24}$, which allowed us to use the same 5 nm AuNPs functionalized with $X_{24,comp}$ for all assemblies. The resulting assemblies are shown in Figure 1. Samples were subsequently imaged using dry AFM in tapping mode (Nanoscope IIIa with a Multimode head and NT-MDT NSG30 tips from Nanoscience Instruments, Inc.). We found that functionalized particles avoid attachment if the adjacent binding sites are closer than ∼20−30 nm apart (center-to-center), as expected for DNA-functionalized particles with negative surface charge (see discussion in ref 28).

We enlarged the size of AuNPs bound to origami templates by reducing silver ions from solution (see Figure 2). The AuNP assemblies adsorbed on silicon substrates were metallized by applying a commercially available microscopic staining kit (HQ-Silver, Nanoprobes, Inc.), which we used previously for fabrication of silver nanowires.[29] The metallization procedure was performed at room temperature inside a red-light illuminated dark room. Equal volumes of the three kit components (initiator, moderator, and activator) were mixed. Conveniently, the reaction proceeded at a slow rate that allowed us to easily control the amount of deposited metal by varying the metallization time. The metallization process was halted by a brief immersion and rinsing of the samples in deionized water. The SEM images in panels A−D of Figure 2 show the growth of NPs bound to the four corners of the origami template and metallized for different times. The measured size of the NPs as a function of metallization time is plotted in Figure 2E.

Figure 3 shows the successful fabrication of metallic structures based on the seed particle assemblies of Figure 1B−D, resulting in rings, pairs of parallel bars, and H shapes. In these structures, the metallization times are long enough and the seed particles are placed close enough to fuse the particles together. Although not all of the binding sites were occupied by AuNPs, as shown in Figure 1, the programmed structures such as H shapes or rings were still formed, as clearly shown in Figure 3. Typically, the center-to-center distance between the seed AuNPs was ∼20 nm, and the metallization times were ∼10 min. The metallic lines formed from four seed particles along the origami side had to be roughly 50 nm thick in order to appear contiguous in SEM images (see Figure 3B).

The narrowest width of a continuous metallic line is limited by the distance between neighboring AuNP seeds. Smaller interparticle distance would reduce the metallization time required to fuse the seeds, thereby decreasing the width of the resultant metallic structures. However, in our experience, the seed particles avoid attaching close to each other. The AuNP−DNA conjugates can probably be brought closer together by reducing the bare particle size, by decreasing the length of the DNA sequence, and by changing the buffer's ionic concentration to reduce the effective particle size.

While the observed amount of successfully assembled structures (see Figure 3) appears encouraging, there are many parameters one could still optimize to increase the overall yield even further, among them the design of the binding sites on the DNA origami, the concentrations of the DNA origami and the AuNP−DNA conjugates, the parameters that control the surface attachment, and the metallization protocol.

In conclusion, we have demonstrated that complex metallic nanostructures can be assembled programmatically using DNA templates, DNA functionalization of seed nanoparticles, and metallization via silver reduction chemistry. We expect that our results will represent an enabling step in fabrication of a wide range of components for nanoelectronic and plasmonic applications.

## ■ ASSOCIATED CONTENT

**ⓢ Supporting Information.** Details of the DNA sequences that were used in this work and a detailed description of AuNP-

DNA conjugate preparation and filtration. This material is available free of charge via the Internet at http://pubs.acs.org/.

## ■ AUTHOR INFORMATION

### Corresponding Author
*E-mail: thomas.labean@duke.edu; gleb@phy.duke.edu.

### Author Contributions
#These authors contributed equally to this work.

## ■ REFERENCES

(1) Seeman, N. C. *Annu. Rev. Biochem.* **2010**, *79*, 65–87.

(2) Samano, E. C.; Pilo-Pais, M.; Goldberg, S.; Vogen, B. N.; Finkelstein, G.; LaBean, T. H. *Soft Matter* **2011**, *7*, 3240.

(3) Rothemund, P. W. K. *Nature* **2006**, *440*, 297–302.

(4) Voigt, N. V.; Torring, T.; Rotaru, A.; Jacobsen, M. F.; Ravnsbaek, J. B.; Subramani, R.; Mamdouh, W.; Kjems, J.; Mokhir, A.; Besenbacher, F.; Gothelf, K. V. *Nat. Nanotechnol.* **2010**, *5*, 200–203.

(5) Maune, H. T.; Han, S.; Barish, R. D.; Bockrath, M.; Goddard, W. A., III; Rothemund, P. K.; Winfree, E. *Nat. Nanotechnol.* **2010**, *5*, 61–66.

(6) Venkataraman, S.; Dirks, R. M.; Rothemund, P. W. K.; Winfree, E.; Pierce, N. A. *Nat. Nanotechnol.* **2007**, *2*, 490–494.

(7) Gu, H.; Chao, J.; Xiao, S.; Seeman, N. C. *Nature* **2010**, *465*, 202–205.

(8) Wickham, S. F. J.; Endo, M.; Katsuda, Y.; Hidaka, K.; Bath, J.; Sugiyama, H.; Turberfield, A. J. *Nat. Nanotechnol.* **2011**, *6*, 166–169.

(9) Sharma, J.; Chhabra, R.; Andersen, C. S.; Gothelf, K. V.; Yan, H.; Liu, Y. *J. Am. Chem. Soc.* **2008**, *130*, 7820–7821.

(10) Hung, A. M.; Micheel, C. M.; Bozano, L. D.; Osterbur, L. W.; Wallraff, G. M.; Cha, J. N. *Nat. Nanotechnol.* **2010**, *5*, 121–126.

(11) Ding, B.; Deng, Z.; Yan, H.; Cabrini, S.; Zuckermann, R. N.; Bokor, J. *J. Am. Chem. Soc.* **2010**, *132*, 3248–3249.

(12) Pal, S.; Deng, Z.; Ding, B.; Yan, H.; Liu, Y. *Angew. Chem., Int. Ed.* **2010**, *49*, 2700–2704.

(13) Kershner, R. J.; Bozano, L. D.; Micheel, C. M.; Hung, A. M.; Fornof, A. R.; Cha, J. N.; Rettner, C. T.; Bersani, M.; Frommer, J.; Rothemund, P. W. K.; Wallraff, G. M. *Nat. Nanotechnol.* **2009**, *4*, 557–561.

(14) Braun, E.; Eichen, Y.; Sivan, U.; Ben-Yoseph, G. *Nature* **1998**, *391*, 775–778.

(15) Gu, Q.; Haynie, D. T. In *Annual Review of Nano Research*; Cao, G., Brinker, C. J., Eds.; World Scientific Publishing Company, Inc.: Hackensack, NJ, 2008; Vol. 2, pp 217-245.

(16) Yan, H.; Park, S. H.; Finkelstein, G.; Reif, J. H.; LaBean, T. H. *Science* **2003**, *301*, 1882–1884.

(17) Park, S. H.; Yan, H.; Reif, J. H.; LaBean, T. H.; Finkelstein, G. *Nanotechnology* **2004**, *15*, S525–S527.

(18) Park, S. H.; Barish, R.; Li, H.; Reif, J. H.; Finkelstein, G.; Yan, H.; LaBean, T. H. *Nano Lett.* **2005**, *5*, 693–696.

(19) Liu, J.; Geng, Y.; Pound, E.; Gyawali, S.; Ashton, J. R.; Hickey, J.; Woolley, A. T.; Harb, J. N. *ACS Nano* **2011**, *5*, 2240–2247.

(20) Park, S.; Taton, T. A.; Mirkin, C. A. *Science* **2002**, *295*, 1503–1506.

(21) Weizmann, Y.; Patolsky, F.; Popov, I.; Willner, I. *Nano Lett.* **2004**, *4*, 787–792.

(22) Huang, Y.; Chiang, C.; Lee, S. K.; Gao, Y.; Hu, E. L.; Yoreo, J. D.; Belcher, A. M. *Nano Lett.* **2005**, *5*, 1429–1434.

(23) Gu, Q.; Cheng, C.; Haynie, D. T. *Nanotechnology* **2005**, *16*, 1358–1363.

(24) Wilner, O. I.; Shimron, S.; Weizmann, Y.; Wang, Z.; Willner, I. *Nano Lett.* **2009**, *9*, 2040–2043.

(25) Schreiber, R.; Kempter, S.; Holler, S.; Schüller, V.; Schiffels, D.; Simmel, S. S.; Nickels, P. C.; Liedl, T. *Small* **2011**, *7*, 1795–1799.

(26) Loweth, C. J.; Caldwell, W. B.; Peng, X.; Alivisatos, A. P.; Schultz, P. G. *Angew. Chem., Int. Ed.* **1999**, *38*, 1808–1812.

(27) Zanchet, D.; Micheel, C. M.; Parak, W. J.; Gerion, D.; Alivisatos, A. P. *Nano Lett.* **2001**, *1*, 32–35.

(28) Sharma, J.; Chhabra, R.; Liu, Y.; Ke, Y.; Yan, H. *Angew. Chem., Int. Ed.* **2006**, *45*, 730–735.

(29) Park, S. H.; Prior, M. W.; LaBean, T. H.; Finkelstein, G. *Appl. Phys. Lett.* **2006**, *89*, 033901.